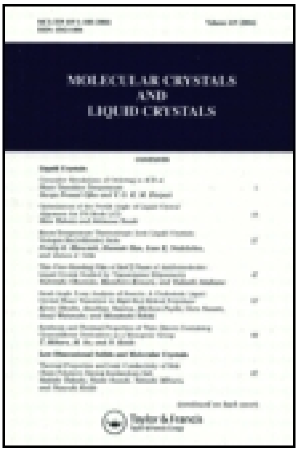

Molecular Crystals and Liquid Crystals
Publication details, including instructions for authors and subscription information:
http://www.tandfonline.com/loi/gmcl20

Redox Reactivity of Methylene Blue Bound in Pores of UMCM-1 Metal-Organic Frameworks

Jonathan E. Halls [a], Charles Y. Cummings [a], Jay Ellis [a], Luke L. Keenan [a], Dongmei Jiang [a], Andrew D. Burrows [a] & Frank Marken [a]
[a] Department of Chemistry, University of Bath, Claverton Down, Bath, BA2 7AY, UK

To cite this article: Jonathan E. Halls, Charles Y. Cummings, Jay Ellis, Luke L. Keenan, Dongmei Jiang, Andrew D. Burrows & Frank Marken (2012): Redox Reactivity of Methylene Blue Bound in Pores of UMCM-1 Metal-Organic Frameworks, Molecular Crystals and Liquid Crystals, 554:1, 12-21

To link to this article: http://dx.doi.org/10.1080/15421406.2012.632738

Mol. Cryst. Liq. Cryst., Vol. 554: pp. 12–21, 2012
Copyright © Taylor & Francis Group, LLC
ISSN: 1542-1406 print/1563-5287 online
DOI: 10.1080/15421406.2012.632738

Redox Reactivity of Methylene Blue Bound in Pores of UMCM-1 Metal-Organic Frameworks

JONATHAN E. HALLS, CHARLES Y. CUMMINGS,
JAY ELLIS, LUKE L. KEENAN, DONGMEI JIANG,
ANDREW D. BURROWS, AND FRANK MARKEN*

Department of Chemistry, University of Bath, Claverton Down,
Bath BA2 7AY, UK

Redox processes were studied in the pores of a crystalline UMCM-1 metal organic framework (MOF) material. Methylene blue was employed as an absorbed redox active dye component. From the change in coloration during dye adsorption, it was concluded that an essentially irreversible adsorption process with high pore loading of the resulting MOF structure occurred. The adsorbed methylene blue remained redox active in the MOF pores and there was no evidence of significant losses during extended redox cycling. Due to the size of the pores, the reactivity of the pore-bound methylene blue is closely related to that expected for methylene blue in an aqueous solution. A study of the effect of solution pH on the voltammetric responses revealed an interesting gradual change in electrical pore conductivity form conducting poorly under acidic conditions to conducting very well under alkaline conditions. This is interpreted in terms of charge transport via single-electron hopping conduction in pores. An estimate of the apparent charge diffusion coefficient at pH 7, $D_{app} = 1.4 \times 10^{-15}$ m^2s^{-2}, is obtained. Potential applications of the new family of redox active hybrid MOF materials are indicated.

Keywords Carbon dioxide; coordination polymers; electrolyte; electron transfer; diffusion; ion conduction; junction; metal-organic frameworks; MOF; pore; pH; sensors; voltammetry

Introduction

The structural family of metal-organic frameworks (MOFs [1]) is rapidly expanding with new structural building blocks being developed [2] and better crystallographic characterisation tools for these complex ordered materials becoming available [3]. The ability of MOFs to adsorb gaseous guest molecules, in particular CO_2, has been widely reported [4] and several cases of larger guest molecule incorporation are known [5]. One particularly interesting type of guest molecules is redox active ferrocenes [6] or redox active heteroaromatics, which can be regarded as "molecular wire" elements to allow electrochemical processes to be driven and studied within the nanopore environments in MOFs.

There is good precedence for the adsorption of dye molecules into MOFs. $[Zn_4O(btb)_2]$ (MOF-177, btb = 1,3,5-benzenetribenzoate) has been shown to absorb Astrazon Orange R, Nile Red, Reichardt's dye, and 4-dimethylamino-4'-nitrostilbene [7,8], whereas

---

*Address correspondence to Frank Marken, Department of Chemistry, University of Bath, Claverton Down, Bath BA2 7AY, UK. E-mail: F.Marken@bath.ac.uk

$[Zn_4O(ndc)(btb)_{4/3}]$ (DUT-6, ndc = 2,6-naphthalenedicarboxylate) has also been shown to absorb Reichardt's dye [9]. The selective absorption of dyes into MOF pores of different sizes has been postulated as a means of separation [10]. In some cases, absorption into the MOFs is limited, but dyes can still be included into MOFs by co-precipitation [11,12]. For example, fluorescein only diffuses into the outer layer of $[Zn_4O(bdc)_3]$ (MOF-5, bdc = 1,4-benzenedicarboxylate), but when introduced into the reaction mixture it is incorporated throughout the crystals [11].

Methylene blue (MB) is a redox active dye that has previously been included into MOFs, although redox properties of the host-guest system have not been investigated. MB was shown to absorb into MOF-5 as part of a study into 'micropatterning' MOFs [13], and its absorption into $[Fe_3O(bdc)_3(DMF)_3][FeCl_4]$ (MOF-235) has led to suggestions that MOFs can be used to remove pollutants from contaminated water [14]. MB has also been shown to absorb into nanoparticulate MOFs containing lanthanides and fluorene-based dicarboxylates [15]. Furthermore, some MOFs have been demonstrated to effectively photocatalyse MB degradation, presumably via initial absorption [16]. In a recent zeolite-based report [17], a structurally related methylene blue dye has been shown to bind into a mesoporous host, whilst maintaining its electrochemical and electrocatalytic activity for ascorbic acid electroanalysis. Work on electrochemical applications of methylene blue intercalated into porous α-$Zr(HPO_4)_2$ host has been reported [18,19].

We have previously shown that $[Zn_4O(bdc)(btb)_{4/3}]$ UMCM-1 [20] is a good framework for electrochemical studies in MOFs, with a demonstration that covalently-bound ferrocene groups, attached by post-synthetic modification, show reversible redox behaviour [21]. However, degradation of MOF structures during redox cycling accompanied by loss of redox activity is commonly observed, particularly in aqueous environments. In this paper, we report the interesting case of stable redox cycling behaviour of MB absorbed into UMCM-1. Fig. 1 shows the methylene blue molecular structure in relation to the UMCM-1

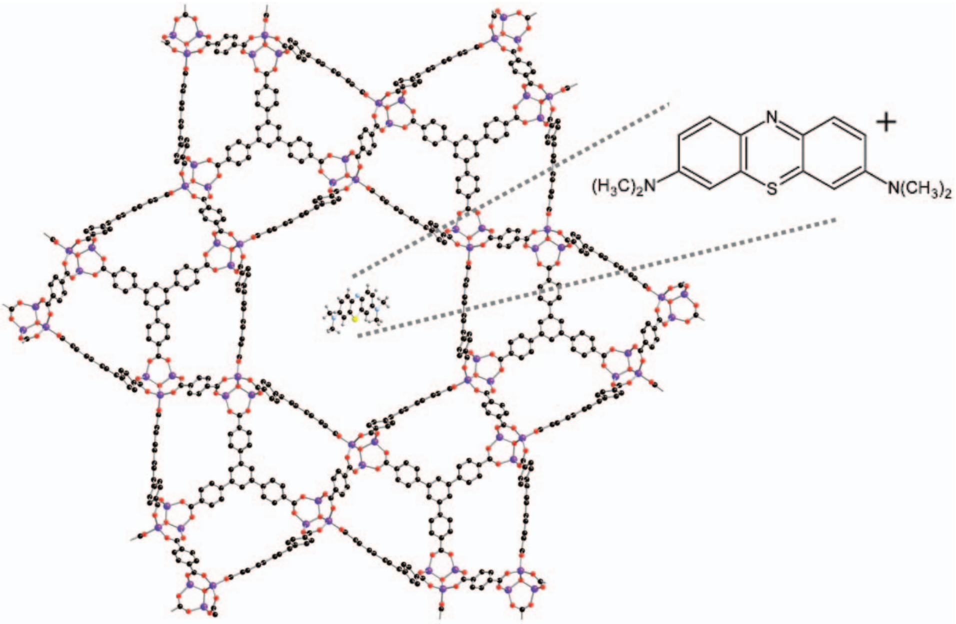

Figure 1. Representation of the UMCM-1 molecular structure [20] with different types of pores and methylene blue molecular structure to size.

pore environment. Due to the pore size methylene blue can be absorbed effectively and can also be contained in an environment that still resembles the aqueous solution phase.

The reduction and back-oxidation of methylene blue is demonstrated immersed in aqueous media and as a function of pH. A mechanism for the pore redox processes based on single-electron hopping is proposed and implications for future applications of redox-active host-guest MOF materials are also discussed.

Experimental Details

Chemical Reagents

[$Zn_4O(bdc)(btb)_{4/3}$], UMCM-1, was prepared by the method reported by Matzger and co-workers [20]. Methylene blue, acetic acid, sodium hydroxide, potassium phosphate monobasic and potassium phosphate dibasic were obtained from Aldrich and used without further purification. Demineralized and filtered water was taken from a Thermo Scientific water purification system (Barnstead Nanopure) with a resistivity of no less than 18 MΩ cm. Instrumentation

Electrochemical experiments were carried out with an Ivium Compactstat potentiostat system (CompactStat, Ivium Technologies B. V., The Netherlands) in cyclic voltammetry mode. A conventional three-electrode cell with platinum wire counter and KCl-saturated calomel (SCE) reference electrode was employed. The working electrode was a 4.9 mm diameter basal plane pyrolytic graphite (bppg, pyrocarbon, Le Carbone UK Ltd.) electrode. Immobilisation of solid powder samples at the graphite electrode surface was achieved following the method of abrasive microparticle adhesion [22]. Four tin-doped indium oxide (ITO, Image Optics, Basildon, resistivity 15 Ω per square) junction experiments focused ion beam (FIB) machined ITO electrodes were employed [23] (FIB: Ga liquid metal ion source (LMIS), 30 kV, 200 pA ion beam for making an approximately 1 micron deep trench; SEM: Carl Zeiss XB1540) resulting in a ca. 500 nm wide gap or junction.). Prior to voltammetric experiments, solutions were de-aerated with oxygen-free nitrogen (BOC Gases, UK). All experiments were performed in aqueous electrolyte at a temperature of 20°C ± 2°C.

Procedures for Methylene Blue Absorption into UMCM-1

A solution of methylene blue was prepared by dissolving methylene blue (0.106 g, 0.331 mmol) in deionised water (100 cm^3). UMCM-1 or [$Zn_4O(bdc)(btb)_{4/3}$] (0.0155 g, 0.022 mmol) was placed in a vial and steeped in 2 cm^3 of the stock methylene blue solution for five days. The vial was stoppered to prevent evaporation. After this time, the solution was filtered and the resultant dark blue crystal powder was washed with deionised water and DMF. The UV/visible spectrum of the filtrate was used to estimate the uptake of methylene blue into [$Zn_4O(bdc)(btb)_{4/3}$].

Results and Discussion

Absorption of Methylene Blue into Metal Organic Framework UMCM-1

[$Zn_4O(bdc)(btb)_{4/3}$] (bdc = 1,4-benzenedicarboxylate, btb = 1,3,5-benzenetribenzoate), UMCM-1, was prepared from the reaction between zinc(II) nitrate and a mixture of H_2bdc and H_3btb following the previously reported method [20]. The identity of the product was confirmed by powder X-ray diffraction. The samples were activated by exchanging the included solvent by dichloromethane, then placing them under a vacuum at room temperature for 2 h.

Absorption of methylene blue was carried out by soaking the activated UMCM-1 crystals in an aqueous solution of methylene blue for 5 days, after which the crystals were separated by filtration and washed with distilled water. During the soaking period, the crystals changed colour from colourless to dark blue. Slices through the crystals demonstrated that the colour change occurred throughout, and was not just limited to the surfaces. After multiple washings with water, very little dye leached out of the crystals. The methylene blue uptake process leads to a reduction in the quality of the UMCM-1 crystals, preventing single crystal analysis from being undertaken on the product. However, SEM images in Fig. 2 show crystalline materials with up to 10 μm size. No significant changes before or after reaction with methylene blue occurred.

In order to calculate the concentration of the solution, UV/visible spectroscopic analysis of the methylene blue solution following uptake into the UMCM-1 sample and alkaline digestion was used, in conjunction with measurements on samples of the known methylene blue concentration. From this, it is estimated that the uptake is approximately 0.14 g g^{-1}, equivalent to 0.45 molecules of methylene blue per [$Zn_4O(bdc)(btb)_{4/3}$] formula unit. This suggests a high level of methylene blue binding and a close interaction of methylene blue molecules within the porous structure (vide infra).

Voltammetric Characterisation of Methylene Blue—UMCM-1 I.: Reversible Processes in UMCM-1 Pores

Initial voltammetric experiments were carried out in aqueous phosphate buffer solution at pH 7 (not shown). The blue MB-UMCM-1 powder was immobilised at the bppg electrode surface and investigated by potential cycling over a potential range from +0.2 to −0.6 V vs. SCE. A well-defined and reversible reduction response was observed with a midpoint potential of ca. $E_{mid} = \frac{1}{2}(E_p^{ox} + E_p^{red}) = -0.26$ V vs. SCE. When investigating the effect of the scan rate, it became obvious that in a phosphate buffer, the MB-UMCM-1 system

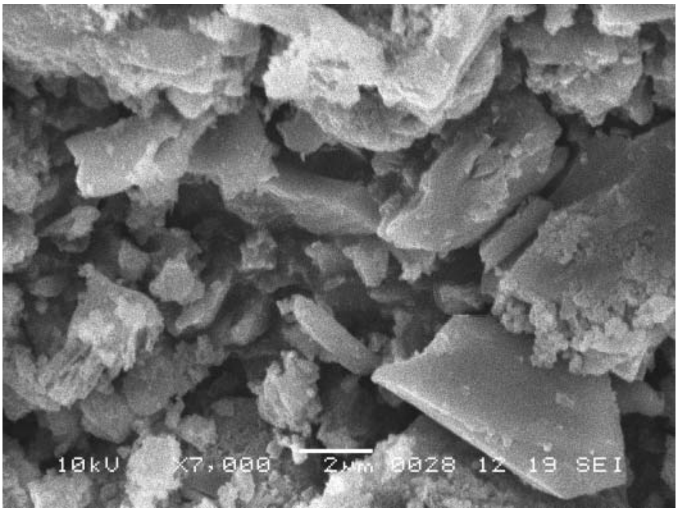

Figure 2. SEM image of UMCM-1 following uptake of MB.

is chemically unstable and slowly transformed during redox cycling. This was deduced from a broadening of the peak shape and from a gradual shift of the E_{mid} potential to more positive potentials. A likely chemical transformation is one from MOF to $Zn_3(PO_4)_2$ via gradual ligand substitution. Therefore, all further experiments were conducted in aqueous acetate buffer.

Fig. 3A shows a typical set of voltammetric responses obtained for MB-UMCM-1 immobilised at a bppg electrode and immersed into 0.1 M acetate solution. The reduction

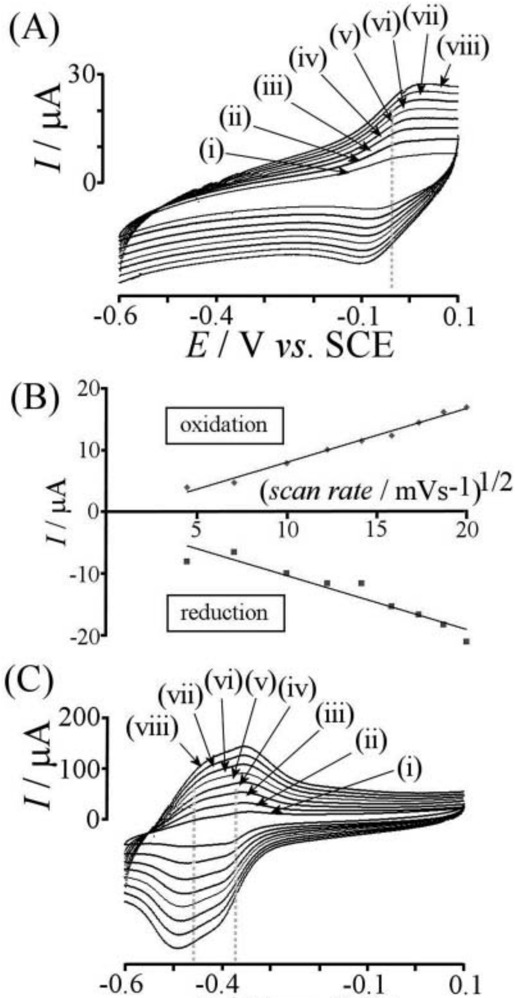

Figure 3. (A) Cyclic voltammograms (scan rates (i) 50, (ii) 100, (iii) 150, (iv) 200, (v) 250, (vi) 300, (vii) 350, and (viii) 400 mVs-1) for the reduction and back-oxidation of MB-UMCM-1 immobilised at a bppg electrode and immersed in aqueous 0.1 M acetate buffer pH 2.2. (B) Plot of the anodic and cathodic peak currents versus square root of scan rate. (C) Cyclic voltammograms (scan rates (i) 50, (ii) 100, (iii) 150, (iv) 200, (v) 250, (vi) 300, (vii) 350, and (viii) 400 mVs-1) for the reduction and back-oxidation of MB-UMCM-1 immobilised at a bppg electrode and immersed in aqueous 0.1 M acetate solution pH 11.3.

and back-oxidation were stable during extended potential cycling and the effect of scan rate was investigated. The plot in Fig. 3B indicates an approximately linear increase in peak current with a square root of scan rate consistent with an increase in charge as the scan rate decreases. This behaviour could be associated with a diffusion process, for example slow charge diffusion across crystal surfaces or into the MB-UMCM-1 bulk material (vide infra).

The midpoint potential for the MB redox process in Fig. 3A is very similar to that described in literature for methylene blue reduction in aqueous media [24]. Therefore, a mechanism may be proposed (Eq. 1), ignoring the added complexities introduced by dimerization and the charge transport in the MOF pores (vide infra).

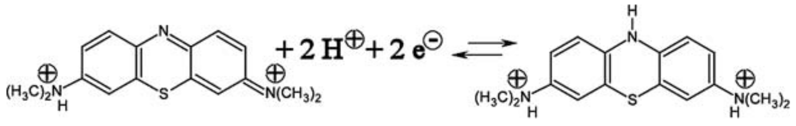

(1)

When changing the pH of the acetate electrolyte solution, several important changes are observed. A gradual shift of the midpoint potential for the voltammetric response with ca. 59 mV per pH unit consistent with equation 1 is observed (see Fig. 4B). At a pH of approximately 7, the voltammetric signals splits into two equivalent reductions and back-oxidation responses (see Fig. 3C). This behaviour is indicative with the presence of a stable radical intermediate (also observed in aqueous solution [25,26]). The overall mechanism for this reduction in aqueous media involves only overall one proton (equation 2), but it is likely to require a second charge compensating cation in the MOF pores.

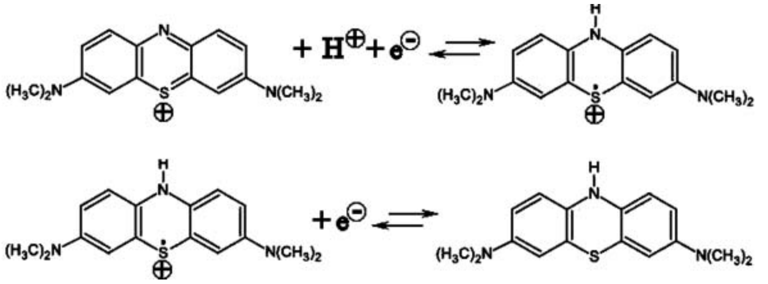

(2)

The pK_A values for leuco-methylene blue in aqueous environments are reported as 5.0 and 5.9 [27] and a similar value can be expected here for the methylene blue adsorbed into MOF pores. A comparison of voltammetric responses for pH 2.2 to 11.3 is shown in Fig. 4A. The broadening of the voltammetric response is clearly observed at pH 7 and therefore the effect of the pK_A of methylene blue on the reaction pathway in the MOF pores is confirmed.

The increase of the peak currents with increasing pH was also observed. The diffusion nature of the electron transport within MB-UMCM-1 at pH 2.2 suggests that only a fraction of the redox active material is accessible at conventional scan rates. The increase in current must therefore reflect an increase in the apparent diffusion coefficient for charge diffusion in MOF pores. The mechanism described in equation 1 (for acidic conditions) requires two electrons, which, in a charge hopping process, has to be accomplished in two consecutive steps. The availability of a one-electron reduced intermediate is important. In contrast, the mechanism described in equation 2 (alkaline conditions), consists of two consecutive one-electron transfers and therefore charge hopping in the MOF pores is more facile.

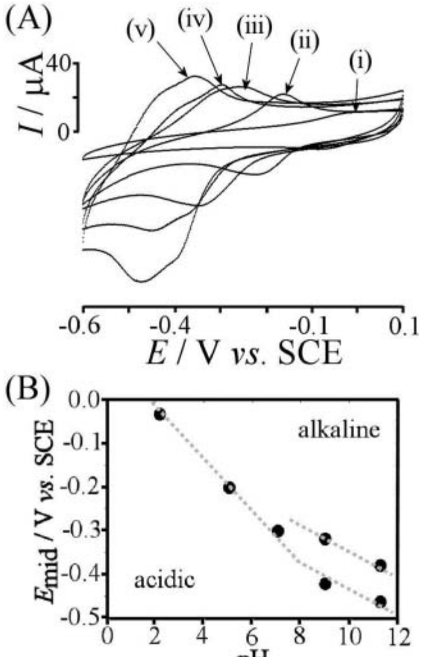

Figure 4. (A) Cyclic voltammograms (scan rates 0.1 Vs-1) for the reduction and back-oxidation of MB-UMCM-1 immobilised at a bppg electrode and immersed in aqueous 0.1 M acetate solution at (i) pH 2.2, (ii) pH 5.0, (iii) pH 7.0, (iv) pH 9.0, and (v) pH 11.3. (B) Plot of the midpoint potentials versus pH.

Voltammetric Characterisation of Methylene Blue—UMCM-1 II.: Charge Transport in UMCM-1 Pores

In order to obtain additional information about the charge transport phenomena in UMCM-1 MOF pores, tin-doped indium oxide (ITO) junction experiments were conducted. MB-UMCM-1 particles were readily dispersed into demineralised water and then deposited onto tin-doped indium oxide (ITO) electrodes. A special ITO electrode has been focused-ion-beam-machined (FIB) to provide a thin ca. 500 nm wide gap (see Fig. 5A and 5B) [23]. One side of this electrode is employed as a working electrode (generator electrode), whereas the second side is employed in constant potential mode (collector electrode, here fixed at 0.0 V vs. SCE). The time delay in the collector current with respect to the generator current allowed for the charge transport processes across the gap (through the MB-UMCM-1 material) to be investigated.

The adhesion of MB-UMCM-1 to ITO is not very strong, but current responses for the generator electrode consistent with data in Fig. 4A were obtained and the corresponding collector current trace was recorded. A hysteresis effect was observed [28] as a function of scan rate and the corresponding analysis allowed the apparent diffusion coefficient for the coupled electron and ion hopping process to be estimated as $D_{app} = 0.0071 \times \frac{v\delta^2 F}{\Delta E_H RT} \approx 1.4 \times 10^{-15}\ m^2 s^{-1}$ at pH 7 (in this expression the apparent diffusion coefficient D_{app} is given by the scan rate v, the width of the gap δ, the Faraday constant F, the gas constant R, the absolute temperature T, and the hysteresis parameter ΔE_H). This value is consistent

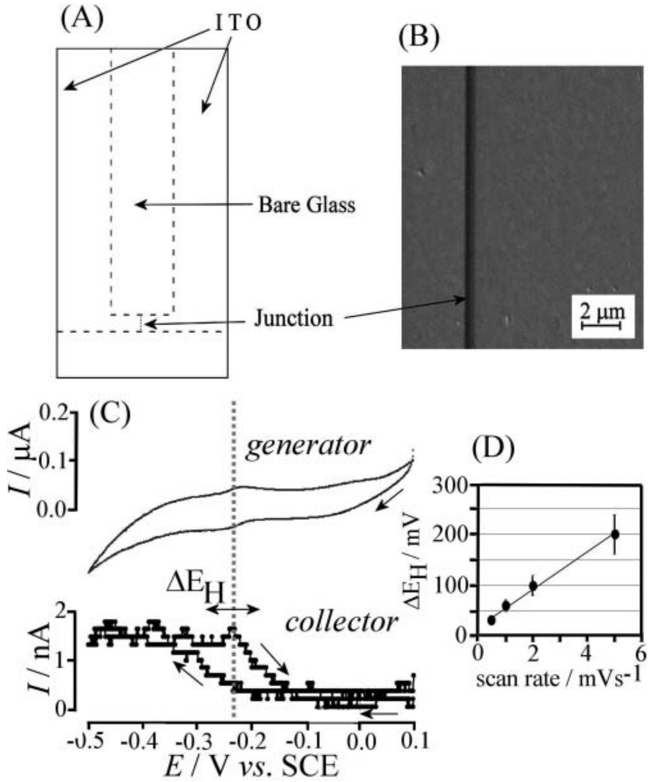

Figure 5. (A) Schematic drawing of the ITO junction electrode. (B) SEM image of the junction with approximately $\delta = 500$ nm gap. (C) Cyclic voltammograms (scan rate 2 mVs^{-1}) for the reduction and back oxidation of methylene blue in UMCM-1 immobilised onto an ITO junction electrode and immersed in 0.1 M phosphate buffer pH 7. Both generator (scanning) and collector (fixed at 0.0 V vs. SCE) current are shown. (D) Plot of the hysteresis voltage ΔE_H as a function of scan rate (20% errors estimated).

with a very slow diffusion-like transport process, either through the bulk of MB-UMCM-1 or, more likely, across the surface of MB-UMCM-1 (see Fig. 6). Unfortunately, the effect of pH on this measurement was not experimentally accessible due to the poor adhesion of MB-UMCM-1 at the ITO electrode surface. New and improved methods for junction

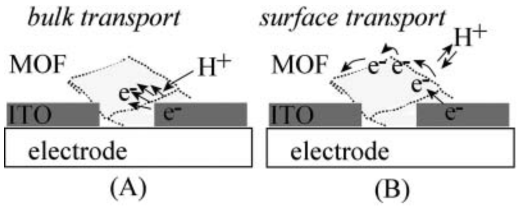

Figure 6. Schematic drawing of MOF junction conductivity effects based on (A) bulk transport of electrons and protons and (B) surface process of electron coupled to proton binding.

measurements are under development to further resolve the charge transport rate and the mechanism as a function of pH.

Conclusions

It has been shown that UMCM-1, a Zn-based MOF, allows adsorption of the dye methylene blue into pores within the structure. Reliable evidence shows that methylene blue retains its electrochemical activity even when bound inside of the MOF host structure, but electron hopping conduction is affected by the pH of the aqueous electrolyte solution surrounding the MOF microparticles. The improved internal charge transport in alkaline environments has been explained based on faster single-electron hopping transport in pores. A first estimate for charge mobility at the surface of MB-UMCM-1 crystals was obtained with junction measurements. In the future, better methods for the determination of pH dependent properties of this class of porous crystalline materials will be required. Co-adsorption effects will be studied, for example in the case of a redox system and $CO_{2,}$ to create artificial reaction environments (similar to those in enzymes) to convert CO_2 via electrochemical reduction.

Acknowledgments

J.E.H. thanks the University of Bath and the EPSRC for a PhD stipend (Nanotechnology grand challenge: EP/H046305/1). Dr. Suguo Huo and Dr. Paul Warburton are gratefully acknowledged for allowing access to the EPSRC FIB service at UCL. C.Y.C. thanks the EPSRC for a studentship.

References

[1] Meek, S. T., Greathouse, J. A., & Allendorf, M. D. (2011). *Adv. Mater.*, *23*, 249.
[2] Burrows, A. D. (2011). *Cryst. Eng. Comm.*, *13*, 3623.
[3] Tan, J. C., & Cheetham, A. K. (2011). *Chem. Soc. Rev.*, *40*, 1059.
[4] Farha, O. K., & Hupp, J. T. (2010). *Acc. Chem. Res.*, *43*, 1166.
[5] Schröder, F., & Fischer, R. A. in Schröder, M. (ed.) (2010). *Topics in Current Chemistry*, *293*, 77.
[6] Meilikhov, M., Yusenko, K., & Fischer, R. A. (2010). *Dalton Trans.*, *39*, 10990.
[7] Chae, H. K., Siberio-Pérez, D. Y., Kim, J., Go, Y., Eddaoudi, M., Matzger, A. J., O'Keeffe, M., & Yaghi, O. M. (2004). *Nature*, *427*, 523.
[8] Choi, J. R., Tachikawa, T., Fujitsuka, M., & Majima, T. (2010). *J. Phys. Chem. Lett.*, *1*, 1101.
[9] Klein, N., Senkovska, I., Gedrich, K., Stoeck, U., Henschel, A., Mueller, U., & Kaskel, S. (2009). *Angew. Chem. Int. Ed.*, *48*, 9954.
[10] Jiang, H.-L., Tatsu, Y., Lu, Z.-H., & Xu, Q. (2010). *J. Am. Chem. Soc.*, *132*, 5586.
[11] Ma, M., Gross, A., Zacher, D., Pinto, A., Noei, H., Wang, Y., Fischer, R. A., & Metzler-Nolte, N. (2011). *Cryst. Eng. Comm.*, *13*, 2828.
[12] Fang, Q.-R., Zhu, G.-S., Jin, Z., Ji, Y.-Y., Ye, J.-W., Xue, M., Yang, H., Wang, Y., & Qiu, S.-L. (2007). *Angew. Chem. Int. Ed.*, *46*, 6638.
[13] Han, S., Wei, Y., Valente, C., Forgan, R. S., Gassensmith, J. J., Smaldone, R. A., Nakanishi, H., Coskun, A., Stoddart J. F., & Grzybowski, B.A. (2011). *Angew. Chem. Int. Ed.*, *50*, 276.
[14] Haque, E., Jun J. W., & Jhung, S. H. (2011). *J. Hazard. Mater.*, *185*, 507.
[15] Zhang, X., Ballem, M. A., Ahrén, M., Suska, A., Bergman, P., & Uvdal, K. (2010). *J. Am. Chem. Soc.*, *132*, 10391.
[16] Mahata, P., Madras G., & Natarajan, S. (2006). *J. Phys. Chem. B*, *110*, 13759.
[17] Sohrabnezhad, S., & Pourahmad, A. (2007). *Electroanalysis*, *19*, 1635.
[18] Pessoa, C. A., Gushikem, Y., & Kubota, L. T. (1997). *Electroanalysis*, *9*, 800.

[19] Cooper, J. A., Woodhouse, K. E., Chippindale, A. M., & Compton, R .G. (1999) *Electroanalysis*, *11*, 1259.

[20] Koh, K., Wong-Foy, A. G., & Matzger, A. J. (2008). *Angew. Chem. Int. Ed.*, *47*, 677.

[21] Halls, J. E., Hernán-Gómez, A., Burrows A. D., & Marken, F. (2011). Dalton Trans., DOI:10.1039/C1DT10734H.

[22] Bond, A. M., & Marken, F. (1994). *J. Electroanal. Chem.*, *372*, 125.

[23] Cummings, C. Y., Wadhawan, J. D., Nakabayashi, T., Haga, M. A., Rassaei, L., Dale, S. E. C., Bending, S., Pumera, M., Parker, S. C., & Marken, F. (2011) *J. Electroanal. Chem.*, *657*, 196.

[24] Sagara, T., & Niki, K. (1993). *Langmuir*, *9*, 831.

[25] Sagara, T., Iizuka, J., & Niki, K. (1992). *Langmuir*, *8*, 1018.

[26] Nicolai, S. H. D., Rodrigues, P. R. P., Agostinho, S. M. L., & Rubim, J. C. (2002). *J. Electroanal. Chem.*, *527*, 103.

[27] Wopschal, R. H., & Shan, I. (1967). *Anal. Chem.*, *39*, 1527.

[28] Vuorema, A., Meadows, H., Bin Ibrahim, N., Del Campo, J., Cortina-Puig, M., Vagin, M. Y., Karyakin, A.A., Sillanpää, M., & Marken, F. (2010). *Electroanalysis*, *22*, 2889.